

## Supplementary Information

### Quantitative analysis of $^{14}\text{N}$ Quadrupolar Couplings Using Proton Detected $^{14}\text{N}$ Solid-State NMR

James A. Jarvis<sup>a</sup>, Maria Concistre<sup>b</sup>, Ibraheem M. Haies<sup>b,c</sup>, Richard W. Bounds<sup>b</sup>,  
Ilya Kuprov<sup>b</sup>, Marina Carravetta<sup>b</sup>, Philip T.F. Williamson<sup>a\*</sup>

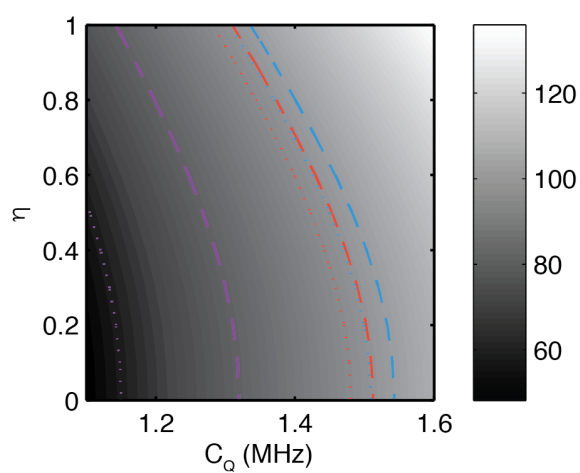
<sup>a</sup>Centre for Biological Sciences, University of Southampton,  
SO17 1BJ, Southampton, United Kingdom.

<sup>b</sup>School of Chemistry, University of Southampton,  
SO17 1BJ, Southampton, United Kingdom.

<sup>c</sup>Department of Chemistry, College of Science,  
University of Mosul, Mosul, Iraq.

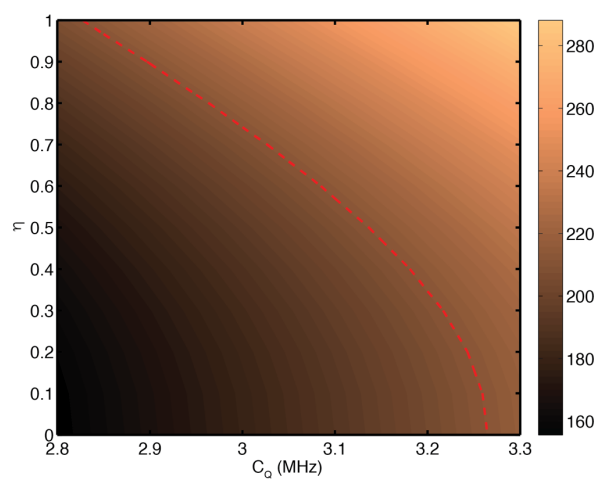
\*Corresponding author: [P.T.Williamson@soton.ac.uk](mailto:P.T.Williamson@soton.ac.uk)

## Supplementary Figure S1



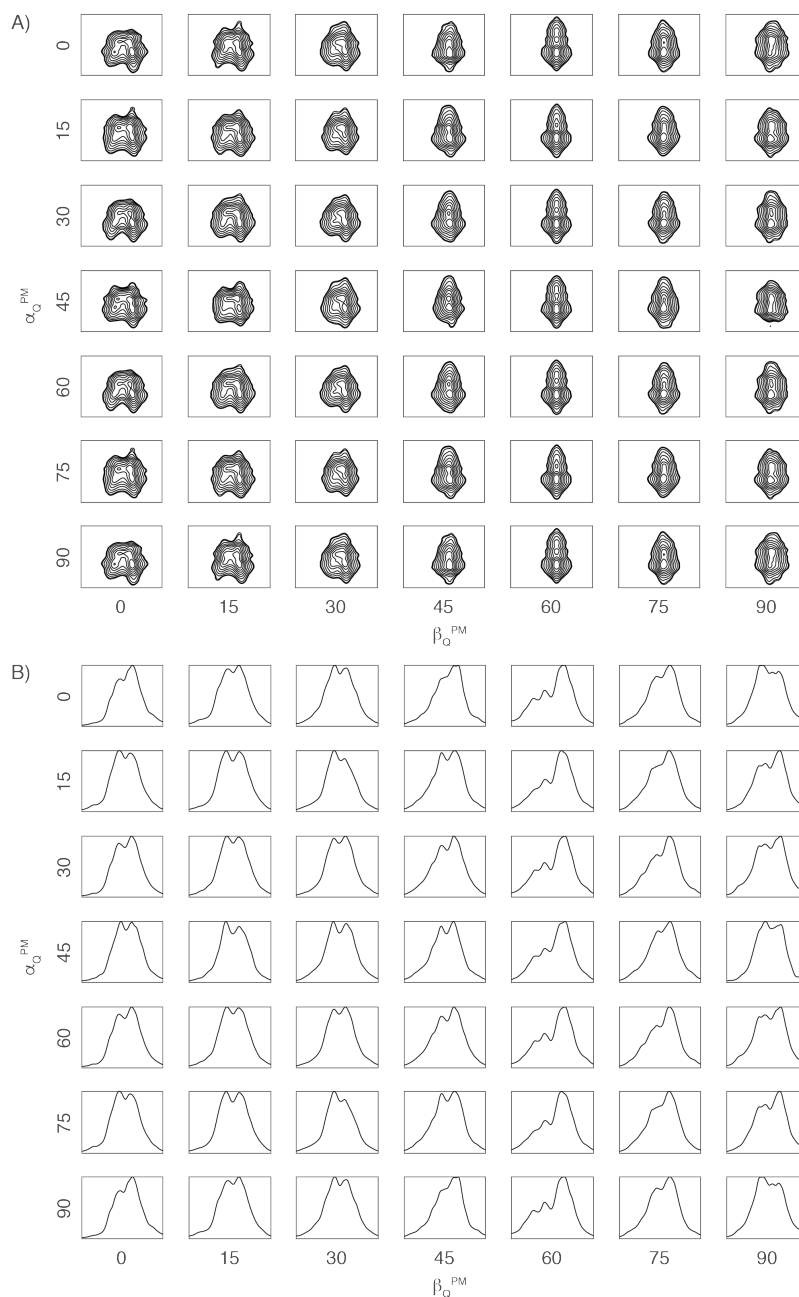
**Supplementary Figure S1.** Plot of  $\delta_{CS}^{iso}$  as a function of  $C_Q$  and  $\eta$  at 14.1T. The  $\delta_{CS}^{iso}$  is plotted in ppm as a function of  $C_Q$  and  $\eta$ , calculated from Equation 1. Plot is for a magnetic field of 14.1T. Dotted and dashed lines indicate the experimentally determined and calculated values for the  $\delta_{CS}^{iso}$ , respectively, of  $-\text{NH}_3^+$ , (purple),  $\text{N}\epsilon$  (blue) and  $\text{N}\delta$  (red) sites in His.HCl.H<sub>2</sub>O.

## Supplementary Figure S2



**Supplementary Figure S2.** Plot of  $\delta_{CS}^{iso}$  as a function of  $C_Q$  and  $\eta$  at 20.T. The  $\delta_{CS}^{iso}$  is plotted in ppm as a function of  $C_Q$  and  $\eta$ , calculated from Equation 1. Dashed lines indicate the experimentally determined values for the  $\delta_{CS}^{iso}$  of the amide nitrogen in NAV.

### Supplementary Figure S3



**Supplementary Figure S3.** Simulations of 2D  $^1\text{H}/^{14}\text{N}$  correlation spectrum of NAV showing influence of relative orientations ( $\alpha_Q^{\text{PM}}$ ,  $\beta_Q^{\text{PM}}$ , 0) of the quadrupolar interaction and the  $^{14}\text{N}$ - $^1\text{H}$  dipolar coupling tensors ( $C_Q=3.2$  MHz,  $\eta=0.32$ , CSA omitted) on lineshape (A,  $^1\text{H}$  x-axis 8 to 10 ppm,  $^{14}\text{N}$  y-axis 250 to 400ppm) and the corresponding skyline projections of the  $^{14}\text{N}$  dimension. (B, normalized to maximum intensity, and plotted between 250 and 400 ppm). Spectra were simulated for a field of 19.96T with a spinning speed of 78 kHz. Simulations were performed with a rotor grid rank of 55 and summed over 1202 powder points and processed with 200 Hz linebroadening in both dimensions.

## Supplementary Figure S4



**Supplementary Figure S4.** Simulations of 2D  $^1\text{H}/^{14}\text{N}$  correlation spectrum of NAV showing influence of relative orientations ( $\alpha_Q^{\text{PM}}$ ,  $\beta_O^{\text{PM}}$ , 0) of the quadrupolar interaction and the  $^{14}\text{N}$ - $^1\text{H}$  dipolar coupling tensors ( $C_Q=3.2$  MHz,  $\eta=0.32$ , with CSA included as described in Table 1) on lineshape (A,  $^1\text{H}$  x-axis 8 to 10 ppm,  $^{14}\text{N}$  y-axis 250 to 400ppm) and the corresponding skyline projections of the  $^{14}\text{N}$  dimension. (B, normalized to maximum intensity, and plotted between 250 and 400 ppm). Spectra were simulated for a field of 19.96T with a spinning speed of 78 kHz. Simulations were performed with a rotor grid rank of 55 and summed over 1202 powder points and processed with 200 Hz linebroadening in both dimensions.